E3S Web of Conferences **397**, 01002 (2023) https://doi.org/10.1051/e3sconf/202339701002
Mathematical Models and Methods of the Analysis and Optimal Synthesis of the Developing Pipeline and Hydraulic Systems 2022

Universal Gas-Liquid Flow Pattern Map and Its Use on Closure Relationship Selection

Leonid Korelstein[2], *Eduardo* Pereyra[1]

[1] McDougall School of Petroleum Engineering, The University of Tulsa, Tulsa, OK 74104, United States,
[2] 2Piping Systems Research & Engineering Co, 7 Plekhanova Street, Moscow, 111141, Russia

Abstract. Mechanistic modelling is a common approach to predict design parameters such as flow pattern, pressure drop, or liquid holdup in gas-liquid flow in pipes. This approach starts with the application of continuity and momentum balance and required supplementary relationships to close the system of the equations. These additional equations are also called closure relationships which are developed with experimental results for given conditions. These relationships evolved with time as researchers acquired experimental data under different conditions. Unfortunately, new closures are developed for the new conditions rather than universal relationships that can cover a wider set of conditions. This situation generates the need for a methodology that allows the inclusion of newly develop closures to increase the accuracy of the unified mechanistic models. This paper starts with a description of all the available two-dimension maps that can facilitate the visualization of the data. This allows the determination of regions where a particular set of closures minimize the discrepancy between calculated and measured parameters. This paper proposes a simplification of a modern solution to provide a simpler way to visualize the regions corresponding to a set of equations. The final proposed solution reveals a substantial reduction of the average discrepancy of the unified mechanistic model by selecting the most appropriate closures.

1. Introduction.

The flow of gas and liquid in pipes presents an interesting phenomenon related to the distribution of the phases in the pipe. The different ways that the gas and liquid distribute in the pipe are called flow patterns which affect the pressure drop, liquid holdup, solid deposition, corrosion, flow-induced vibrations, and other related parameters. Historically, the two-dimensional mapping of the different flow patterns has been critical for proper system design. One of the most popular maps has been proposed in 1974 by Mandhane et al. [1] which is presented in Figure 1(a) for horizontal flow. In these maps, the flow pattern regions are described in superficial liquid velocity (v_{SL}) vs. superficial gas (v_{SG}) coordinates. The superficial velocity is the velocity as one phase flow alone in the pipe (the phase flow rate over the area of the pipe). For low superficial gas velocities, the observed flow pattern is stratified flow with the smooth interface (SS). As the gas flow rate increases, the interaction

between the gas and the liquid generates stable waves defining a stratified wavy flow patterns (SW). Further increase in the gas flow rate promotes the initiation of droplet generation from the crest of the waves. The generated droplets are deposited in the pipe wall creating a liquid film. As the gas flow rate keeps increasing, the film generated in the upper pipe wall gets thicker and establishes the transition to annular flow (AN). Coming back to stratified smooth (SS), if the liquid flow rate increases at a constant gas flow rate, the liquid level tends to increase to a point that any perturbation in the flow could grow and block the pipe cross-sectional area generating elongated bubble flow (EB). This flow pattern is characterized by a periodic flow of gas and liquid body in the pipe. The liquid body does not present any recirculation in the front, so no dispersed gas is entrained and observed in the liquid body. From EB conditions, an increase of gas flow rate, at a constant liquid flow rate, also increases the velocity of the liquid slug to a point that a vortice appears in the front entraining gas that flows through the slug towards the tail of the slug. This flow pattern is called slug flow (SL) and the main difference with EB is the presence of the vortice and the entrained gas in the slug body. Finally, at a large liquid flow rate, the turbulence in the liquid is capable of dispersing all the gas generating a dispersed bubble flow (DB). On the transition between slug and annular flow, churn (CH) and pseudo slug (PSL) are observed. These two flow patterns are characterized by large coherent structures with gas-passing troughs. Churn flow is usually observed near vertical flow while pseudo slugs are observed below 75°.

The main disadvantage of Mandhane et al. (1974) is that only works for a given set of fluid properties and pipe geometry. The transition lines in Figure 1(a) was developed for air-water flow at atmospheric conditions and pipe diameters from 1.27 to 5.1 cm. Different transition lines need to be generated if a larger pressure or diameter wants to evaluate. Other researchers have tried to extend the applicability of the flow pattern maps by including dimensionless numbers. Govier and Aziz (1972) [2] propose a correction factor for the superficial velocities (see Figure 1(b)) based on air and water as a reference. The map was developed for vertical flow and the corrections factors for the gas and liquid superficial velocities are given as follows:

$$X = \left(\frac{\rho_G}{\rho_A} \right)^{1/3}, \tag{1}$$

$$Y = \left(\frac{\rho_L}{\rho_A} \frac{\sigma_{WA}}{\sigma_{LG}} \right)^{1/4}, \tag{2}$$

where ρ_G is the gas density, ρ_L is the liquid density, ρ_A is the air density at atmospheric conditions, σ_{LG} is the surface tension between liquid and gas, and σ_{WA} is the surface tension between air and water and atmospheric conditions. With the inclusion of the fluid properties, Govier and Aziz (1972) expected that the corrected flow pattern could be extended from water at an atmospheric environment to other operational conditions. Griffith and Wallis (1961) [3] also proposed the use of two dimensionless numbers to describe the transition to annular flow (see Figure 1(c)). Experimental observations showed that this transition can be defined by the non-slip void fraction ($v_{SG}/(v_{SG}+v_{SL})$) and the square of the mixture Froude number as follows:

$$Frm^2 = \frac{v_m^{\ 2}}{g\, d}, \tag{3}$$

where v_m is the mixture velocity ($v_{SL}+v_{SG}$), g is the gravitational acceleration and d is the pipe diameter.

Another dimensionless flow pattern map was proposed by Baker (1953) [4]. The author used the mass flow rate of gas and liquid (GG and GL). He also proposed two corrections factors as described in (see Figure 1(d)) defined as follows:

$$\lambda = \left(\frac{\rho_G / \rho_A}{\rho_L / \rho_W} \right)^{1/2}, \tag{4}$$

$$\psi = \frac{\sigma_{WG}}{\sigma_{LG}} \left(\frac{\mu_L / \mu_W}{\rho_L / \rho_W} \right)^{1/2}. \tag{5}$$

These two correction factors are based on the air and water properties at standard conditions. Other attempts at flow pattern visualization include design parameters such as pressure gradient. Figure 2 showed the flow pattern for horizontal and vertical flow proposed by Govier and Aziz (1972) [5].

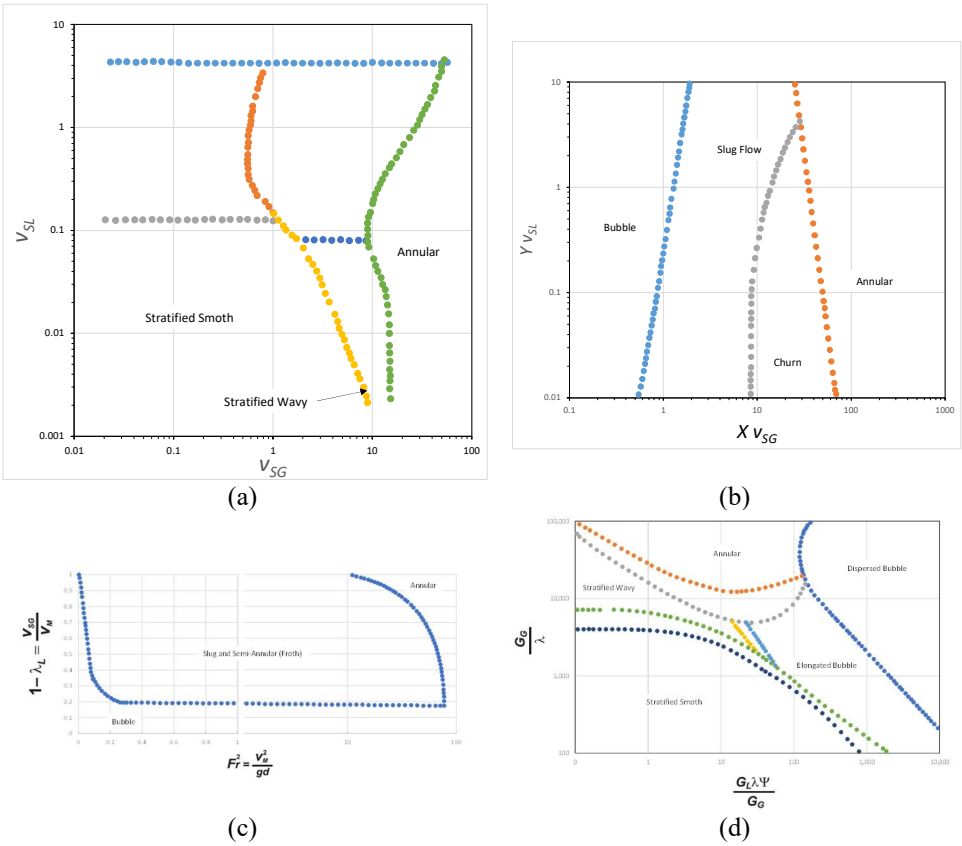

Figure 1, Empirical Flow Pattern Maps.

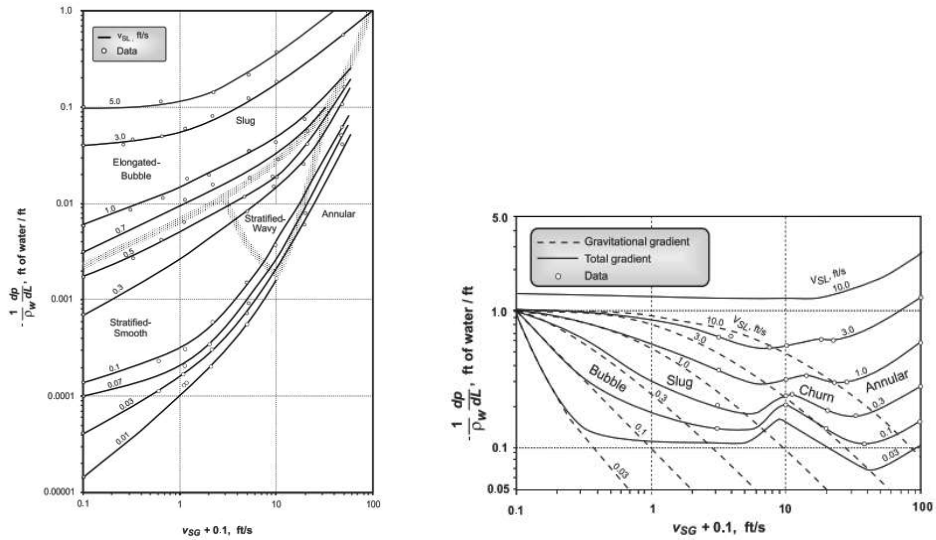

(a) (b)

Figure 2, Empirical Flow Pattern Maps.

Taitel and Dukler (1976) [6] proposed the first flow pattern dimensionless map base on a mechanistic approach. The authors started with the analysis of the stratified liquid level by applying continuity and momentum balance for the gas and liquid phase. To simplify the equation, Taitel and Dukler assumed: 1) steady state 2) pressure drop in that gas and liquid section is the same, 3) gas and liquid wall shear stress can be estimated with single phase flow equation using a hydraulic diameter, 4) liquid average velocity is negligible as compared to the gas velocity and 5) the interfacial friction factor is equal to the gas-wall friction factor. After these assumptions, the two-fluid model can be reduced to a combined momentum equation that can be written in a dimensionless form:

$$\left[\left(\tilde{v}_G\,\tilde{d}_G\right)^{-0.2}\tilde{v}_G{}^2\left(\frac{\tilde{S}_G}{\tilde{A}_G}+\frac{\tilde{S}_I}{\tilde{A}_L}+\frac{\tilde{S}_I}{\tilde{A}_G}\right)\right]-X_{LM}{}^2\left[\left(\tilde{v}_L\,\tilde{d}_L\right)^{-0.2}\tilde{v}_L{}^2\frac{\tilde{S}_L}{\tilde{A}_L}\right]-4\,Y_{LM}=0 \tag{6}$$

where v, A, S, and d represent velocity, areas, perimeters, and hydraulic diameter respectively. The subindex L and G represent the gas and liquid phase. The symbol ˜ indicates the dimensionless quantities. The velocity, areas, perimeters, and hydraulic diameter equation are a unique function of the dimensionless stratified liquid level (h_L/d) as follows:

$$Aux = 2\times h_L / d - 1\,, \tag{7}$$

$$\tilde{S}_I = \sqrt{1-Aux^2}\;,\;\; \tilde{S}_G = \cos^{-1}(Aux)\,,\;\; \tilde{S}_L = \pi - \tilde{S}_G\,, \tag{8}$$

$$\tilde{A}_G = 0.25\times\left(\cos^{-1}(Aux) - Aux\times\tilde{S}_I\right),\;\; \tilde{A}_L = 0.25\times\pi - \tilde{A}_G \tag{9}$$

$$\tilde{v}_L = \frac{0.25\times\pi}{\tilde{A}_L}\,,\;\; \tilde{v}_G = \frac{0.25\times\pi}{\tilde{A}_G}\,, \tag{10}$$

$$\tilde{d}_L = \frac{4\times \tilde{A}_L}{\tilde{S}_L},\ \tilde{d}_G = \frac{4\times \tilde{A}_G}{\tilde{S}_G + \tilde{S}_I}. \tag{11}$$

The other two parameters in the combined momentum equation (XLM and YLM) correspond to the Lockhart and Martinelli (1949) [7] parameters as follows:

$$X_{LM}{}^2 = \frac{\left[dp/dl\right]_{SL}}{\left[dp/dl\right]_{SG}},\ Y_{LM} = \frac{(\rho_L - \rho_G)\, g \sin(\theta)}{\left[dp/dl\right]_{SG}}. \tag{12}$$

where $[dp/dl]_{SL}$ and $[dp/dl]_{SG}$ are the gas and liquid pressure gradient as each phase flow along in the pipe. As can be seen, these two parameters are a function of fluid properties, operational conditions, pipe diameter, and inclination angle. Based on this, the dimensionless stratified liquid level (h_L/d) can be obtained implicitly from the momentum equation (6). This also indicates that the dimensionless stratified liquid level is a unique function of the Lockhart and Martinelli parameters (X_{LM}, Y_{LM}). Taitel and Dukler presented a simplified Kelvin-Helmholtz analysis to determine the stability of the stratified flow. Based on this, the flow pattern can be classified as stratified (ST) if the following inequality is satisfied:

$$F_{SG}{}^2 \left[\frac{1}{(1-h_L/d)}\frac{\tilde{v}_G{}^2 \tilde{S}_I}{\tilde{A}_G}\right] \geq 1, \tag{13}$$

where the superficial gas Froud number is given by:

$$F_{SG} = \sqrt{\frac{\rho_G}{(\rho_L - \rho_G)}}\frac{v_{SG}}{\sqrt{d\ g}}. \tag{14}$$

The transition from stratified (ST) to non-stratified (Non-ST) is determined by considering the equal sign in equation (13) and the solution is presented in Figure 3(a). To determine if the flow pattern corresponds to stratified smooth (SS) or wavy (SW), Taitel and Dukler modify the Jeffreys (1925) [8] criterion for the wave formation in water interfaces to the pipe flow configuration. The authors suggested that the stratified flow can be classified as wavy (SW) if equation (15) is satisfied, otherwise, the stratified flow should be classified as smooth (SS). The transition line is preened in Figure 3(a) using the dimensionless parameter K to separate stratified smooth from wavy.

$$\underbrace{F_{SG}{}^2 \times \left(\frac{\rho_L \times v_{SL} \times D}{\mu_L}\right)}_{K} \geq \frac{2}{\sqrt{0.01\tilde{v}_L}\ \tilde{v}_G}. \tag{15}$$

If equation (13) is satisfied, the flow pattern could be annular, slug, or dispersed bubble flow. Carrying a force balance between gravity and turbulence, Taitel and Dukler proposed a stability criterium for dispersed bubble flow (DB) as presented in equation (16). The transition line using the dimensionless parameter T is presented in Figure 3(a).

$$\underbrace{\frac{\left[dp/dl\right]_{SL}}{(\rho_L - \rho_G)\, g)}}_{T^2} \geq \left[\frac{8\,\tilde{A}_G}{\tilde{S}_I\, \tilde{v}_L{}^2 \left(\tilde{v}_L \times \tilde{d}_L\right)^{-0.2}}\right]. \tag{16}$$

The remaining transition line (B), corresponds to the transition from slug to annular flow. If equations (13) and (16) are not satisfied, the flow pattern is either slug (SL) or annular flow (AN). For this, if the dimensionless stratified liquid level (hL/d) is less than 0.35 the flow pattern is annular flow, otherwise is slug flow. Since the main postulation of Taitel and

Dukler model is around the stratified liquid level, the flow pattern map presented in Figure 3(a) only applies to horizontal and near horizontal flow (+/-10°). Later, Barnea (1987) [9] extended this mechanistic approach to all inclination angles. Her biggest contribution towards a dimensionless map is the transition from annular to non-annular flow depicted in Figure 3(b). The author carried out a stability analysis of the film which defines the transition (a). Barnea also proposed an additional mechanism on which the liquid holdup in the annular flow should be less than a given threshold (HL< 0.24) defining the transition (b) in Figure 3(b). This map reinforces the importance of the Lockhart and Martinelli parameters to universally represent the flow pattern transition lines.

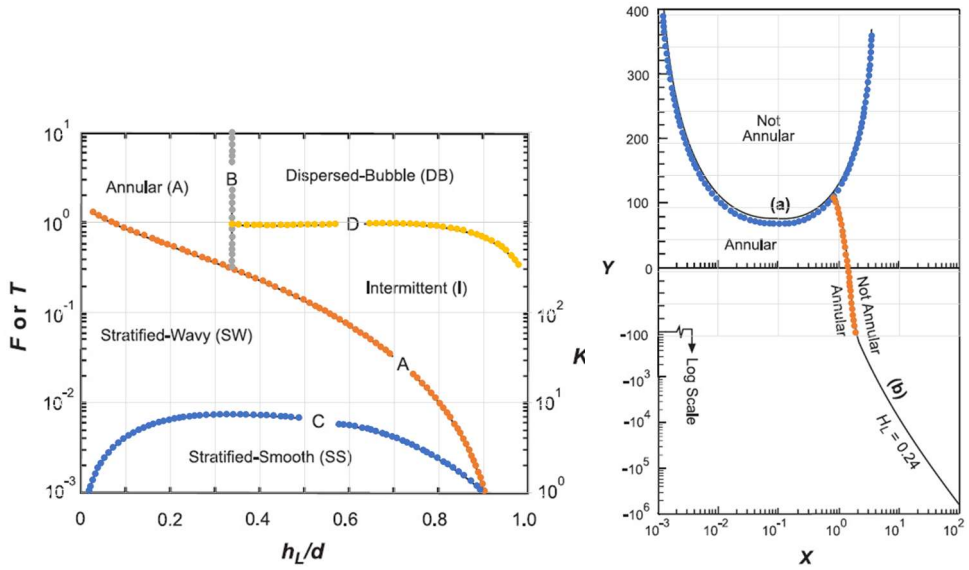

(a) (b)

Figure 3, Mechanistic Based Flow Pattern Maps.

As mentioned before, flow pattern prediction is of critical importance to calculate different design parameters such as pressure gradient and liquid holdup. Mechanistic models have been utilized for flow patterns, pressure drop, and holdup prediction. Zhang et al. (2003) [10] proposed a widely used unified mechanistic model that can be applied to all inclination angles and sets of conditions. The model is based on the stability of slug flow and simultaneously determines the flow pattern, pressure drop, and liquid holdup. The model contemplates continuity and momentum equations for the different gas-liquid flow patterns. A set of independent closure relationships (CLRs) are then required to close the system of equations. The required closures are:

1. Liquid slug length (*Ls*).
2. Slug liquid holdup (H_{LS}).
3. Slug translational velocity (v_T).
4. Drift velocity (v_d).
5. Liquid entrainment (*fe*).
6. Interfacial friction factor (*fi*).

These closure relationships are developed using dedicated experiments to measure the beforementioned parameters. A different set of equations has been proposed in the literature based on the available data. The final accuracy of the mechanistic models depends on the accuracy of the closure relationships. New data and closure relations are continuously developed for a different set of conditions making it difficult for the development of universal

closure relationships to assist the unified model. An alternative way is to develop a methodology to select the best set of closures for a given condition. This will allow the use of newly developed closures as they are developed. Few authors had investigated this problem in the past, Brustur (2015) [11] proposed a polynomial interpolation approach to select the best set of closures for Zhang et al. (2003) unified model using an extended database. Later Babenko and Korelstein (2016) [12] used the TUFFP (2023) database [13] to create a closure relationship selector using the near-neighbor approach. Roullier et al. (2017) [14] utilized a field data set to evaluate the best set of closures for large pipe diameter conditions. Recently, Mohammadi et al. (2019) [15] utilize a genetic algorithm to select the best combination of closure for a given set of conditions. The authors propose the use of the proposed algorithm over a given cluster of data. The publication didn't elaborate on how the data needed to be clustered.

As can be seen, there is a need for a methodology that allows a proper clusterization of the available multiphase flow database to identify regions and set of closures that reduces the discrepancy between measured and predicted parameters such as pressure gradient (dp/dl) and liquid holdup (H_L). For this, it is required a universal flow pattern map that allows the graphical representation of the clusters. Thus, this paper aims to propose a simple and accurate dimensionless flow pattern map and its application for closure relationship selection considering the Zhang et al. (2003) unified model.

2. Proposed Froud dimensionless flow pattern map

From previous 2D dimensionless plots, the most used representation corresponds to Mandhane et al. (1974) [1]. However, the use of superficial velocities in the axis required the definition of the transition lines for a new set of conditions. On the other hand, Taitel and Dukler (1976) [6] map is based on the underlying mechanisms but is infrequently used. The idea is to combine the advantages of both maps and proposed a dimensionless map that can be applied to a larger set of conditions. Following equation (13), the superficial Froude number (F_{SG}) for the Taitel and Dukler (1976) [6] transition from stratified (ST) to non-stratified (Non-ST) and to annular flow can be defined as a unique function of the stratified liquid level ($F_{SG}=f(h_L/d)$). Considering horizontal flow ($Y_{LM}=0$), equation (6) indicates that the stratified liquid level is a unique function of X_{LM} ($h_L/d=g(X_{LM})$). Thus, a transition from stratified flow to non-stratified flow can be written in terms of the superficial gas Froud number and the Lockhart and Martinelli parameter ($F_{SG}=f(X_{LM})$). The Lockhart and Martinelli can be written as:

$$X_{LM}^{\ 2} = \frac{\left[dp/dl\right]_{SL}}{\left[dp/dl\right]_{SG}} = \frac{f_{SL}\,\dfrac{\rho_L\, v_{SL}^2}{2d}}{f_{SG}\,\dfrac{\rho_G\, v_{SG}^2}{2d}}. \tag{17}$$

Assuming fully developed turbulent flow (superficial friction factors are constant and equal) for both phases and multiplying by numerator and denominator by the density differences, gravity, and diameter, the Lockhart and Martinelli parameters simplify to:

$$X_{LM}^{\ 2} = \frac{\left[dp/dl\right]_{SL}}{\left[dp/dl\right]_{SG}} \frac{\left(\dfrac{\rho_L\, v_{SL}^2}{(\rho_L-\rho_G)\,d\;g}\right)}{\left(\dfrac{\rho_G\, v_{SG}^2}{(\rho_L-\rho_G)\,d\;g}\right)} = \frac{F_{SL}^{\ 2}}{F_{SG}^{\ 2}}. \tag{18}$$

So, the transition from stratified to non-stratified and to annular flow in horizontal flow can be simplified to a relationship between the liquid vs. gas superficial Froud number. Figure 4 presents the comparison with experimental data using the horizontal conditions reported by: Abdul-Majeed (1996) [16]; Abduvayt (2003) [17]; Brill et al. (1995) [18]; Fan (2005) [19]; Felizola (1992) [20]; Kokal (1986) [21]; Kouba (1986) [22]; Magrini (2009) [23]; Marcano et al. (1998) [24]; Meng (1999) [25]; Nädler and Mewes (1995) [26]; Roumazeilles et al. (1996) [27]; Vongvuthipornchai (1982) [28]; Vuong (2016) [29]; Wilkens (1997) [30]; Wong and Yau (1997) [31]; Yang (1996) [32]; Zheng (1989) [33]. The data cover pipe diameters from 0.0254 to 0.1524 m, pressure conditions from 1 to 30 bars, and liquid viscosities less than 10 mPa s. The transition lines have been sketched empirically looking for the best transition. The transition (a) separates the stratified points (ST, SW, and SS) from the non-stratified cases (SL, AN, DB). For stratified flow conditions, transition (c) separates stratified smooth form from stratified wavy. Transition (d) separates dispersed bubble from non-dispersed bubble flow. In the middle region (no dispersed and non-stratified flow) transition (b) defines the annular flow region and transition (e) the pseudo slug region. As can be seen, this dimensionless flow pattern map is similar to Mandhane et al. (1974) [1] but allows the scaling up to different pressure and pipe diameters. Such quality permits the use of this graphical representation for the clustering and classification process. This proposed map can be applied to horizontal and low-viscosity liquids (Na<1). Further analysis is required to extend the map for other inclinations and high liquid viscosity conditions.

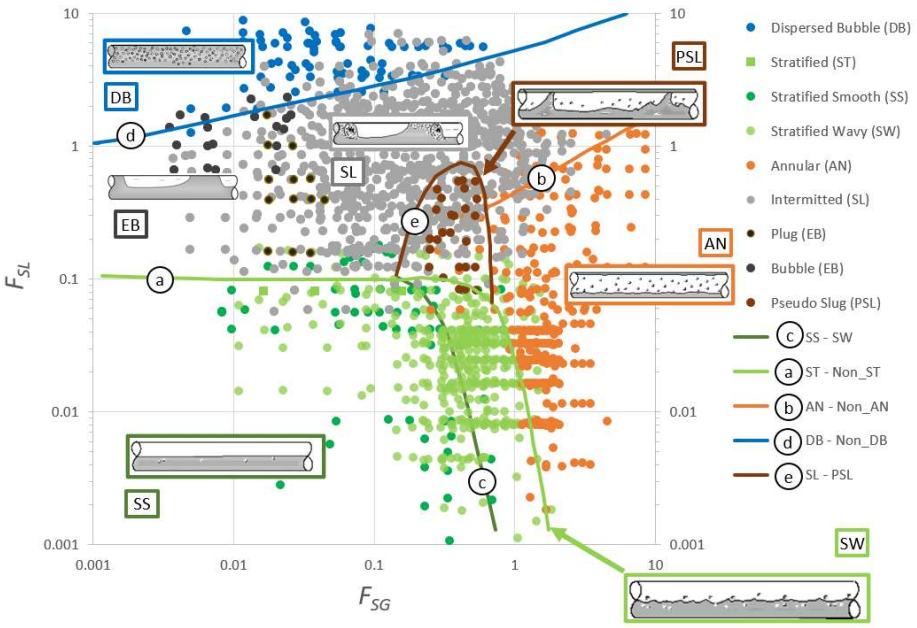

Figure 4, Superficial Froude Numbers Flow Pattern Map for Horizontal Flow and Low Viscosity Liquids (Na<1).

3. Closure relationship selection

For the development of the closure selector, the TUFFP (2023) database [13] has been used. This repository contains measurements of gas-liquid flow in pipes. The data contains fluid properties, operational conditions, and pipe geometries. Also, observed flow patterns, pressure gradient, and liquid holdup are reported. Not all the data sets contain these

measurements. Initially, only horizontal flow is utilized. Since the proposed dimensionless map is more suitable for low-viscosity liquids, the Soto-Cortes et al. (2022) [34] number is used to determine the low-viscosity cases. Based on their observations, the authors proposed that any data point with *Na* number less than one should be classified as low viscosity liquid.

$$Na = \sqrt{\frac{g\,d\left(\rho_L - \rho_G\right)}{\rho_L}}\,\frac{\mu_L}{\sigma}\,. \tag{19}$$

where σ is the surface tension and μ_L is the liquid viscosity. In summary, only data sets for horizontal flow and with *Na*<1 are utilized for the closure relationship selection. Additionally, only data sets with liquid holdup and pressure drop have been included for further analysis. The remaining data sets after the filters are Beggs (1972) [35], Cheremisinoff (1977) [36], Mukherjee (1979) [37], Crowley and Rothe (1988) [38], Andritsos (1986) [39], Kokal (1986) [21], Crowley (1999) [40], Brill et al. (1995) [18], Meng (1999) [25], Tayebi et al. (2000) [41], Abduvayt (2003) [17], Fan (2005) [19], Johnson (2005) [42], Magrini (2009) [23] and Vuong (2016) [29]. There are a total of 1647 points. The gas density varies from 1.13 to 48 kg/m^3. The liquid viscosity raged from 0.7 to 70 mPa s. The smallest pipe diameter is 0.025 m while the largest is 0.17 m. The range of liquid surface tension is from 22 to 73 mN/m.

This data set is used in combination with Zhang et al. (2003) [10] unified model to determine the best set of closures to minimize the discrepancy with the experimental data. The objective function to be minimized consider the combined discrepancy of the holdup and pressure gradient measurements as follows:

$$Obj = \frac{1}{n}\sum_{i=1}^{n}\frac{1}{2}\left[\left|\frac{H_{L\_\exp(i)} - H_{L\_pred(i)}}{H_{L\_\exp(i)}}\right| + \left|\frac{\left[\frac{dp}{dL}\right]_{\exp(i)} - \left[\frac{dp}{dL}\right]_{pred(i)}}{\left[\frac{dp}{dL}\right]_{\exp(i)}}\right|\right]. \tag{20}$$

The slug translational velocity (v_T) and drift velocity (v_d) are closure relationships that do not present large variations. Thus, the closure for translational and drift velocity originally proposed Zhang et al. (2003) [10] will be used in this evaluation. A total of five (5) closures are used for slug length (*Ls*), thirteen (13) relationships are evaluated to slug liquid holdup (H_{LS}), twelve (12) liquid entrainment relationships are considered for liquid entrainment (*fe*), and a total of seventeen (18) for interfacial friction factor (*fi*). Based on this, a total of one thousand four hundred-four (5*13*12*18=14.040) different combinations of closures are evaluated in this study. The value of the objective function (equation (20)) of each of the 1647 points is calculated for all the 1404 sets of closure relationships. Then, the best set of closures is stored for further analysis. The frequency distribution of each data closure set is presented in Figure 5. As can be seen, the five closure sets (Set 0, 1170, 2340, 9360, and 10,530) with the more frequent best performance are related to the entrainment closure (Zhang et al. (2003) [10], Wallis (1969) [43], Paleev and Filippovich (1966) [44], Ousaka et al. (1996) [45], and Al-Sarkhi et al. (2012) [46]). The second-best performance is related to the changes in slug liquid holdup where the best correlations and models (Set 0 and 6) correspond to Zhang et al. (2003) [10], Gomez et al. (2000) [47]. The location of the points corresponding to each of the sets is presented in Figure 6. The original set of correlations or set 0 (Zhang et al. (2003) [10]) is uniformly dispersed along the map. This shows the generality of the selected correlation that is capable of providing fair prediction along the

map. The average discrepancy for Set 0 is about 40%. The regions indicated in the graph for each set of closures have been selected to describe the location with the biggest density of points. Figure 7 presents the proposed set of closure utilization based on the dimensionless map and the database comparison. The value of the objective function for this combination of closure sets reduces to 32.5%. This demonstrates the use of a dimensionless flow pattern to cluster the available experimental data to select the most adequate closure for a given region.

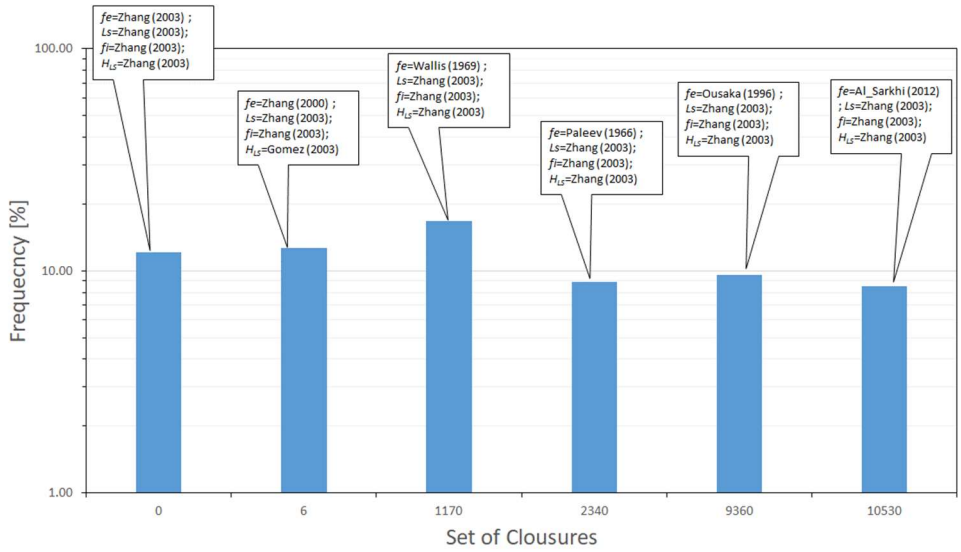

Figure 5, Frequency Distribution for the Best Set of Closures.

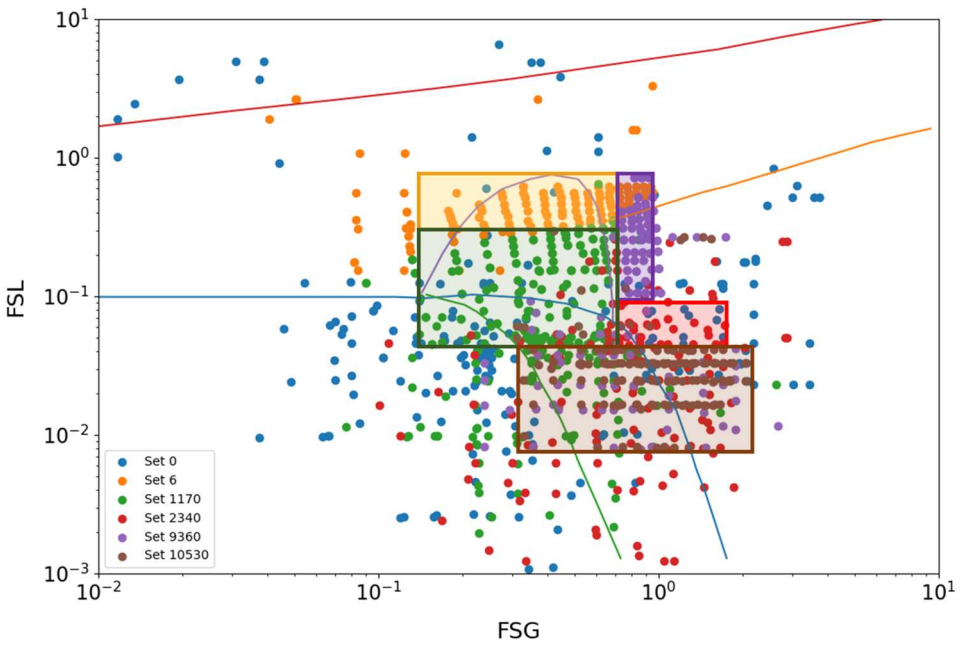

Figure 6, Set of Closure Location in the Map.

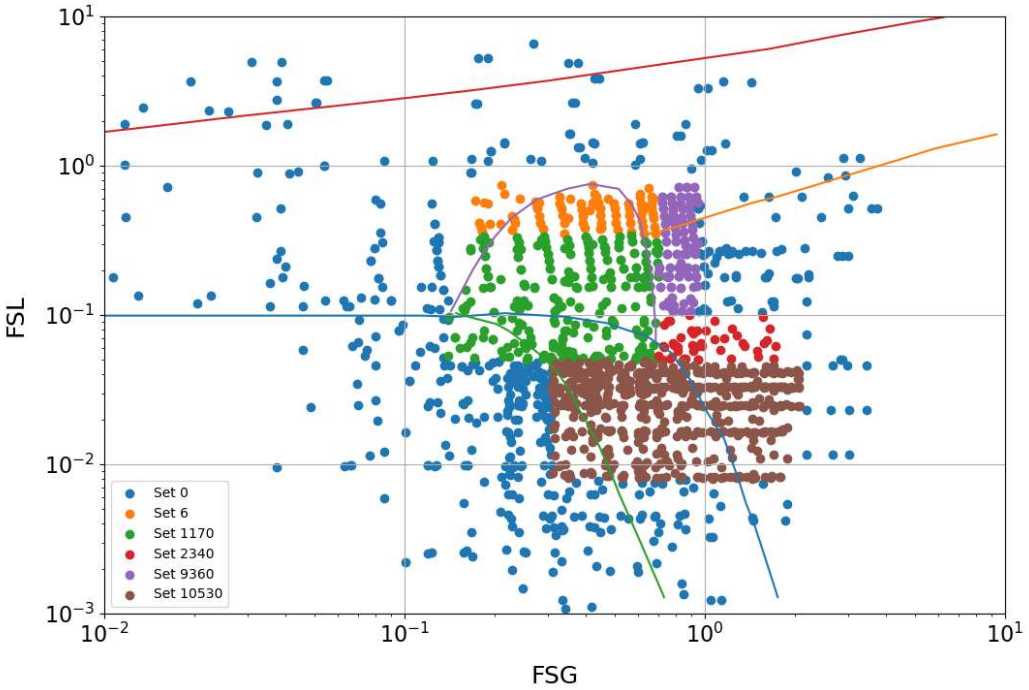

Figure 7, Recommended Set of Closure Utilization in the Map.

4. Conclusions

This paper presents a review of the available 2D dimensionless flow pattern maps for gas-liquid flow. However, the most used representation is based on superficial velocities (Mandhane et al. (1974) [1]) which are made for a specific set of conditions. Modern representations are based on a mechanistic approach (Taitel and Dukler (1976) [6] and Barnea (1987) [9]) but are not widely used. Based on a simplification of the Taitel and Dukler (1976) [6] map, a new dimensionless representation is proposed considering the superficial liquid Froude number vs. the superficial gas Froude number. This map follows the form of Mandhane et al. (1974) [1] facilitating the representation. The new map allows the scalability of different pipe diameters and pressures. The map is evaluated with the TUFFP (2023) [13] database and new flow pattern observation regions are proposed for horizontal and low viscosity (Na<1) conditions.

The map is also utilized to define a procedure for closure relationship selection for the unified model proposed by Zhang et al. (2003) [10]. Translational and drift velocity closures have been kept the same as presented by Zhang et al. (2003) [10] since they don't vary considerably as compared to other closures. A total of 1404 closure sets have been evaluated considering different parameters such as slug length, entrainment, interfacial friction factor, and slug liquid holdup. When compared with the TUFFP (2023) database [13], the entrainment fraction shows to be the most critical relationship. Only the 6 sets with a bigger

impact on the final results were evaluated. The proposed dimensionless map was utilized to define the regions where each closure set should be used. These areas have been selected based on the density of points. As a result, the value of the objective function could be reduced from 80 to 65%. Further analysis is required for larger viscosities and different inclination angles. For that, the current map should be modified to account for such factors.

References

1. Mandhane, JM, GA Gregory, and K. Aziz. J. Multiph. Flow. **1**, 7 (1974)
2. Govier, W. and K. Aziz. *The Flow of Complex Mixtures in Pipes*. (Wiley 1972)
3. Griffith, Peter, and Graham B. Wallis. J Heat Transfer **83**, 3 (1961)
4. Baker, Ovid. Petroleum Branch of AIME, Dallas, Texas, (1953)
5. Govier, W. and K. Aziz. *The Flow of Complex Mixtures in Pipes*. (Wiley 1972)
6. Taitel, Y and Dukler, A. AIChE J. **22**, 1 (1976)
7. Lockhart, R. and Martinelli, R. Chem Eng Prog. 45, 1 (1949)
8. Jeffreys, H. Proceedings of the Royal Society of London. **107**, 742 (1925)
9. Barnea., D. J. Multiph. Flow **13**, 1. (1987)
10. Zhang, H. Wang, Q. Sarica, C and Brill, J. J. Energy Resour. Technol. **125**, 4 (2003)
11. Brustur, A. Curtin University, M Sc These (2015)
12. Babenko, A and Korelstein, L. J Stat Comput Simul. **2**, 83 (2016)
13. TUFFP. 2023. *Gas-Liquid Pipe Flow Data Repository*.
14. Roullier, D. Shippen, M and Adames, P. SPE Annual Technical Conference and Exhibition (2017)
15. Mohammadi, S. Papa, M. Pereyra, E and Sarica, C. International Conference on Data Intelligence and Security, ICDIS. (2019)
16. Abdul-Majeed, G. J. Pet. Sci. Eng. **15**,27 (1996)
17. Abduvayt, P. Arihara, N. Manabe, R and Ikeda, K. J. Jpn. Pet. Inst. **46**, 2 (2003)
18. Brill, J. Chen, T. Flores, J and Marcano, R. Transportation of Liquid in Multiphase Pipelines Under Low Liquid Loading Conditions. Report (1995)
19. Fan, Y. The University of Tulsa. Ph.D. Dissertation (2005)
20. Felizola, H. The University of Tulsa. MS.c Theses (1992)
21. Kokal, S. The University of Calgary. Ph.D. Dissertation (1986)
22. Kouba, Gene. The University of Tulsa. Ph.D. Dissertation (1986)
23. Magrini, K. The University of Tulsa. MS.c Theses (2009)
24. Marcano, R. Chen, T. Sarica, C and Brill, C. Int. Petroleum Conference and Exhibition (1998)
25. Meng, W. The University of Tulsa. MS.c Theses (1999)
26. Nädler, M. and Mewes, D. J. Multiph. Flow. **21**, 2 (1995)
27. Roumazeilles, P. Yang, J. Sarica, C. Chen, X. Wilson, J and Brill, J SPE Prod. Facil **11**, 3(1996)
28. Vongvuthipornchai, S. The University of Tulsa. MS.c Theses (1982)
29. Vuong, D. The University of Tulsa. Ph.D. Dissertation (2016)
30. Wilkens, R. Ohio University. Ph.D. Dissertation (1997)
31. Wong, T. and Yau, Y. ICHMT. **24**, 1:111–18. (1997)
32. Yang, J. The University of Tulsa. Ph.D. Dissertation (1996)
33. Zheng, G. The University of Tulsa. MS.c Theses (1989)
34. Soto-Cortes, G. Pereyra, E and Sarica, C. *Unified Closure Relationship for Slug Liquid Holdup*. The University of Tulsa, Internal Report (2022)
35. Beggs, H The University of Tulsa. Ph.D. Dissertation (1972)
36. Cheremisinoff, N The University of Tulsa. Ph.D. Dissertation (1977)
37. Mukherjee, H. The University of Tulsa. Ph.D. Dissertation (1979)

38. Crowley, C. and Rothe, P. PSIG Annual Meeting. Ontario (1988)
39. Andritsos, N. University of Illinois at Urbana-Champaign. Ph.D. Dissertation (1986)
40. Crowley, C. International Conference of Multiphase Flow, Nice, France. (1999)
41. Tayebi, D. Nuland, S and Fuchs, P. J. Multiph. Flow. **26**, 5 (2000)
42. Johnson, G. University of Oslo. Ph.D. Dissertation . (2005)
43. Wallis, G. B. *One-Dimensional Two-Phase Flow* (McGraw-Hill 1969)
44. Paleev, I. and Filippovich, B. Int. J. Heat Mass Transf. **9**,10 (1966)
45. Ousaka, A. Morioka, I. and Kariyasaki, A. *Nippon Kikai Gakkai Ronbunshu, B Hen/Transactions of the Japan Society of Mechanical Engineers.* **62**,600 (1996)
46. Al-Sarkhi, A. Sarica, C and Qureshi, B. J. Multiph. Flow. **39**,21 (2012)
47. Gomez, L. Shoham, O and Taitel, Y. J. Multiph. Flow. **26**, 3 (2000)